Pyrocumulonimbus Firepower Threshold: a pyrocumulonimbus prediction tool

Kevin Tory, Bureau of Meteorology & Bushfire and Natural Hazards CRC.

Pyrocumulonimbus (fire-induced thunderstorms, pyroCb) are associated with unpredictable changes in fire intensity, spread rates and direction, enhanced ember transport and lightning ignitions. Conventional thunderstorm threats such as downbursts, hail, lightning, and tornadoes may also be present. This paper introduces a pyroCb prediction tool and its application is demonstrated.

In favourable atmospheric conditions, suitably large and hot fires can produce pyroCb cloud in the form of deep convective columns with many similarities to conventional thunderstorms. They may be accompanied by strong inflow, dangerous downbursts and lightning strikes, which may enhance fire spread rates and fire intensity, cause sudden changes in fire spread direction, and the lightning may ignite additional fires. Dangerous pyroCb conditions are not well understood and can be very difficult to forecast.

In recent Bushfire and Natural Hazards CRC (BNHCRC) research, a method for determining how favourable the atmospheric environment is for pyroCb development was developed. This method is combined with a plume-rise model (originally developed for pollutant dispersion prediction) to determine how much heat a fire must produce for pyroCb to develop in a given atmospheric environment. More specifically, this fire heat is the rate at which heat enters the fire plume (which has units of power), often termed the 'power of the fire' or 'firepower'. A theoretical minimum firepower required for pyroCb to develop in a given atmospheric environment is calculated, termed the Pyrocumulonimbus Firepower Threshold (PFT).

Forecast spatial plots of PFT are being trialled that provide an indication of how the favourability of the atmosphere for pyroCb development varies in space and time over typical weather forecast periods. It is anticipated that such plots will provide useful guidance for fire weather forecasters and fire agencies. Preliminary studies have shown that the PFT can vary substantially from day to day, and that days that favour pyroCb formation do not necessarily favour large-hot fires. A PFT-flag is also under development that identifies when both pyroCb and large-hot fires are favourable.

Background - previous BNHCRC research

In previous BNHCRC research an idealized theoretical plume model was introduced (Tory et al. 2018, Tory & Kepert 2018) that can identify at what temperature and pressure (or height) condensation will begin to form in a fire plume. These condensation properties vary according to how much warmer the plume is than the environment (i.e., how buoyant the plume is). Plotted on a thermodynamic diagram, the condensation properties are represented by a single point, termed the Saturation Point (SP), and the SPs for a range of plume buoyancies form a SP curve (Fig. 1, solid blue curve). Each SP curve is unique to an assumed mixed-layer environment comprising constant mixed-layer potential temperature (θ_{ML}, Fig. 1 thick red line) and specific humidity (q_{ML}, Fig. 1 thick pale-blue line), and an assumed fire moisture to heat production ratio (φ). Fortunately, the SP curves are not sensitive to a range of realistic values of φ, and neither is the PFT.

The SP curve defines where a hypothetical ascending plume parcel begins to follow a moist adiabat on a thermodynamic diagram. For pyroCb formation any moist ascending parcel needs to remain buoyant (warmer than the environment, rightmost thin red line in Fig. 1) until it reaches some designated height at which pyroCb is deemed to have been achieved. Here, that height is the so-called electrification level, -20 °C (Fig. 1, pale-blue dashed line). The coolest moist adiabat that satisfies these criteria represents the coolest possible pyroCb plume-element pathway, and thus defines the pyroCb moist-adiabat limit (Fig. 1, yellow curve).

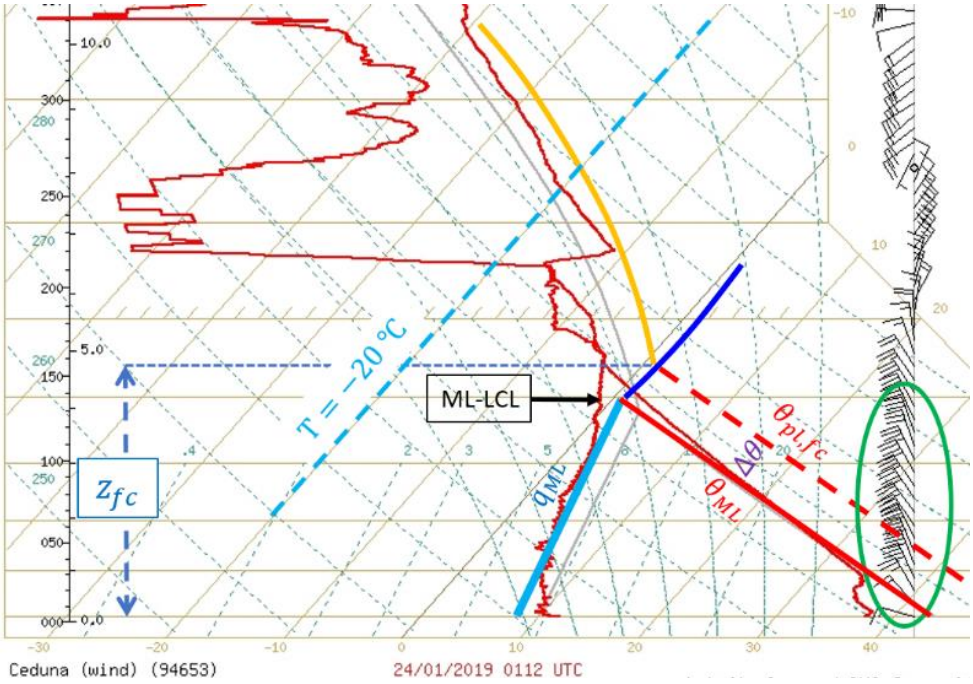

Figure 1: A sample atmospheric sounding (thin red lines and wind barbs) applied to an F-160 thermodynamic diagram, with quantities required for the PFT calculation overlaid: Mixed Layer potential temperature (θ_{ML}, thick red line); Mixed-Layer specific humidity (q_{ML}, thick pale-blue line); Mixed-layer lifting condensation level (ML-LCL, apex of the θ_{ML} and q_{ML} lines); Saturation Point curve (SP curve, blue curve emanating from the ML-LCL); Free-convection moist adiabat (yellow curve); Electrification level ($T = -20$℃, pale-blue dashed line); Free-convection height (z_{fc}, blue dotted line corresponding to the intersection of the SP curve and free-convection moist adiabat); Free-convection plume potential temperature ($\theta_{pl,fc}$, red dashed line); Plume excess potential temperature ($\Delta\theta$, difference between $\theta_{pl,fc}$ and θ_{ML}); and the winds used to calculate the mixed-layer wind speed (U, green ellipse).

Where this moist adiabat and the SP curve meet is the free-convection height limit. Any buoyant plume element that reaches or exceeds this height will, in theory, freely convect to the electrification level. The intersection of these two curves defines the free-convection height (z_{fc}, Fig. 1, fine blue dashed line), which is one of the key inputs to the PFT (see below). Another key PFT input is a measure of the plume-element buoyancy at this height. Specifically, it is the potential temperature difference ($\Delta\theta$) between the plume element at z_{fc} ($\theta_{pl,fc}$) and θ_{ML}, which can easily be read off the thermodynamic diagram (Fig. 1). $\Delta\theta$ is a proxy for the plume buoyancy, and represents the buoyancy required for the plume to overcome any stable layers (inversions) that might inhibit the plume from reaching the electrification level. The third key PFT input is the average mixed-layer windspeed, which can be determined directly from the wind data available or estimated from the winds barbs on the edge of a thermodynamic diagram (Fig. 1, highlighted in the green ellipse).

PFT equations

The PFT is derived from an equation that describes the buoyancy flux distribution along the plume centerline for a Briggs plume (Briggs 1975, 1984) in a constant horizontal wind crossflow (U) and neutrally stable environment (Tory & Kepert 2018, Tory 2018). A schematic representation of a Briggs plume is shown in Fig. 2. The plume geometry is described by two equations, an equation for the plume centreline height (Fig. 2, yellow line) with downwind distance (x),

$$z_c = \left[\left(\frac{3}{2\beta^2}\right)\frac{B_{flux}}{\pi}\right]^{\frac{1}{3}}\frac{x^{\frac{2}{3}}}{U}, \quad 1.$$

and an equation that describes an upright circular plume cross-section,

$$R = \beta z_c. \quad 2.$$

Here B_{flux} is the buoyancy flux at the plume source, which is proportional to the heatflux or firepower entering the plume. β is a constant entrainment coefficient and π is the circle constant. Eq. 2 describes the radius of the dynamic plume (pale blue lines, Fig. 2), which includes the plume gases (internal plume) plus the surrounding environment lifted by the rising plume. The internal plume (dark blue lines, Fig. 2) radius is smaller and is given by,

$$R' = \beta' z_c. \quad 3.$$

Both entrainment parameters (β and β') have been measured in numerous observational and laboratory studies yielding $\beta = 0.6$ and $\beta' = 0.4$ (e.g., Briggs 1975, 1984). The PFT equation is based on buoyancy flux conservation within the internal plume, and thus β' is the appropriate entrainment parameter in the following equations.

Assuming only some fraction of the plume area (α) needs to reach the free-convection height, represented by a fraction of the plume radius, α' (Fig. 2, red arrow), then the plume centreline expressed as a function of the free-convection height becomes,

$$z_c = \frac{z_{fc}}{1+\alpha'\beta'}, \quad 4.$$

and the PyroCb Firepower Threshold becomes,

$$PFT = \left\{\frac{\pi C_p}{R_d}\left[\frac{\beta'}{1+\alpha'\beta'}\right]^2\right\}\left(\frac{P_c}{\theta_{pl,fc}}\right) {z_{fc}}^2 U \Delta\theta_{fc}. \quad 5.$$

Here C_p and R_d are the Specific heat at constant pressure and gas constant for dry air. P_c is the pressure at the plume centreline corresponding to the free-convection height, and $\theta_{pl,fc}$ is the plume potential temperature at the free-convection height (by definition $\theta_{pl,fc} = \theta_{ML} + \Delta\theta$). Equation 5 is a slightly more accurate PFT formulation than that provided in Tory & Kepert (2018). (Note, this work is still under development, and further tuning and changes are likely in the future.)

PFT equation insights

Since the entrainment coefficients (β and β') are constant, the plume centreline height (Eq. 1) at any given downstream distance x is a function of only two variables, the buoyancy flux (B_{flux}), and the background cross-flow wind (U). Considering these variables independently, it is clear that the plume centreline height is much more sensitive to changes in the wind than the firepower. For example, to double the plume height at a given x would require the windspeed to be halved, whereas it would require the firepower to be increased eight times. This result suggests that observed temporal changes in plume height and slope are more likely to be associated with variations in windspeed than fuel type and/or fuel loads.

The curly bracket term in Eq. 5 is constant, and the curved bracket term typically varies by 10% or less, which means the majority of PFT variation comes from the remaining terms: the free convection height, the background wind speed and the plume excess potential temperature (the buoyancy proxy). The relationship between the PFT and each of these three terms makes sense intuitively. The larger the free convection height, the more firepower required for the plume to rise to that height. The greater the windspeed, the more firepower is required to counter the tendency for the plume to be tilted over by the wind. The greater the buoyancy required for the plume to penetrate stable layers or inversions above z_{fc}, the more firepower that is required. The real insight provided by Eq. 5, however, is the relative power of each term and how they combine to determine an overall pyroCb formation threat. For example, if z_{fc} decreases while $\Delta\theta_{fc}$ increases, perhaps with the passage of a cold front or sea breeze, Eq. 5 will determine if the net effect is more or less favourable for pyroCb formation.

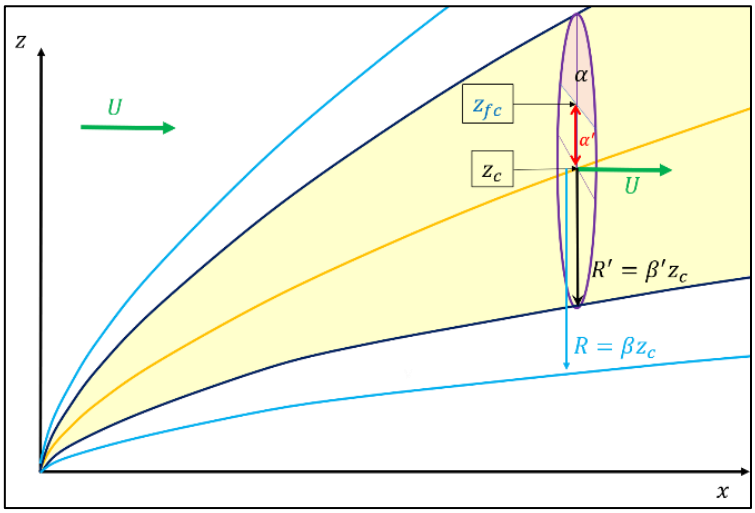

Figure 2: Schematic representation of a Briggs plume, bent-over in the downwind direction (x) by a constant crossflow (U). The internal plume (yellow shading) has a vertical circular cross-section about the plume centreline height (z_c, yellow line) of radius R', which is linearly proportional to the plume centreline height via the constant internal plume entrainment parameter (β'). Similarly, the dynamic plume (inside the pale blue lines) is defined by the dynamic plume radius and entrainment rate, R and β. Only a fraction of the plume area (α) is required to reach the free-convection height (z_{fc}), which can be expressed as a fraction of R' (α').

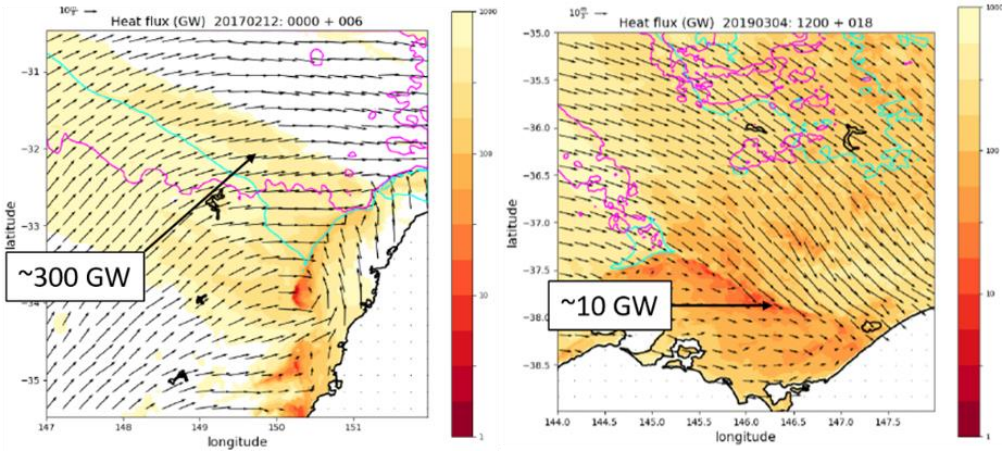

Figure 3: PFT forecasts for two pyroCb events, Sir Ivan (5 PM, 12 February 2017, left) and Licola (5 PM, 5 March 2019, right). The PFT scale is logarithmic (units GW). The wind barbs represent the mixed-layer wind velocity. The PFT label for Sir Ivan points to the fire site, whereas for Licola it points to a minimum value on the wind change that is about to impact Licola.

Results

PFT spatial distributions

Spatial plots of PFT generated from computer forecast models can provide valuable insight into how the pyroCb threat varies in space and time (Fig. 3). The PFT colour scale in Fig. 3 is logarithmic in order to capture the substantial PFT variability at any given time across the landscape. Both cases presented show increased threat near a wind change. This is a very common result. Ahead of the wind change the winds are often very hot and dry (contributing to large z_{fc}) and the windspeeds are often very high (large U), which together contribute to large PFT (Eq. 5) corresponding to highly unfavourable conditions for pyroCb formation. If the wind change brings cooler and moister air to the fire ground (reduced z_{fc}), and a short-term (or longer) lull in the winds (reduced U), conditions become much more favourable for pyroCb formation. Furthermore, a shift in wind direction can lead to increased firepower as long flank fires become head fires.

The two PFT plots in Fig. 3 also demonstrate very large differences in PFT in the vicinity of the fires at the time the pyroCb were observed (about 300 GW for Sir Ivan and 10 GW approaching Licola). This suggests pyroCb formation conditions are much less favourable for the Sir Ivan fire than the Licola fire, since 30 times the firepower would be required in the former than the latter. Indeed, conditions that highly favour pyroCb plume development (high humidity and light winds) do not favour large, hot fires, and vice-versa.

Fire-weather forecasters and fire-behaviour analysts using the PFT diagnostic would require some knowledge of the size and intensity of any going fires to be able to assess pyroCb formation potential. This knowledge is rarely available and will never exist for fires that have yet to be ignited. Without such knowledge they can only identify a relative threat, and the PFT forecast performance cannot be verified.

It may be many years before sufficiently reliable observations of firepower become available to enable a rigorous verification program to be undertaken. In the short term, a dataset of past events could be constructed, to identify fire-types that will produce pyroCb for a specific PFT forecast (eg, a Sir Ivan-scale fire is required for pyroCb to form when the PFT = 300 GW). However, this approach is not ideal because it assumes the yet to be verified PFT is stable and performs consistently across the full breadth of fire weather conditions.

An unverifiable forecast tool such as the PFT has limited prediction value. It must be combined with other information to have value. Ideally, the pyroCb prediction tool would allow forecasters to know that a fire burning in a specific location at a specific time will or will not produce pyroCb.

Returning to Fig. 3 one clear difference between the Sir Ivan and Licola fires is the fire-danger conditions. Sir Ivan had catastrophic fire conditions, which would support a much hotter fire than the very-high fire danger conditions present in Licola. Combining some measure of the fire danger conditions with the PFT could produce a verifiable prediction tool.

PFT-flag formulation

The PFT-flag is designed to represent a ratio of pyroCb plume-development potential (PFT) to fire-intensity potential, to identify when a favourable combination of plume and fire potential is present. For simplicity, the PFT-flag uses only atmospheric variables readily available in Numerical Weather Prediction (NWP) models. The atmospheric components of a variety of fire-weather indices were tested, with the best performing being the product of the Project Vesta (Cheney et al. 2012) and the near-surface windspeed. The main test was for the PFT-flag to produce a similar value for the two extreme cases introduced above, Sir Ivan and Licola. Despite this very rudimentary testing regime the only changes required, after application to more than twenty cases, were the addition of low-wind and low fire-danger limits.

In order to separate the atmospheric component from the fuel components in the Vesta function, two assumptions need to be made. The near-surface windspeed is greater than $5\ km\ hr^{-1}$ ($1.39\ m\ s^{-1}$), and a constant term in the rate-of-spread equation is small compared to the windspeed/fuel term and can be ignored. The latter assumption is good for moderate to high fuel loads. Such fuel loads may be necessary to support deep flaming, observed in pyroCb producing fires (McRae and Sharples 2014). The resulting Vesta atmosphere-only equation can be expressed as,

$$V = 18.35{V_M}^{-1.495}.V_U, \quad 6.$$

where,

$$V_M = \begin{cases} 2.76 + 0.124RH - 0.0187T, \text{Period 1} \\ 3.60 + 0.169RH - 0.0450T, \text{Period 2} \\ 3.08 + 0.198RH - 0.0483T, \text{ Period 3} \end{cases} \quad 7.$$

$$V_U = 1.531(\max(U_{10}, 3.0) - 1.39)^{0.858}. \quad 8.$$

Here V_M and V_U are the fuel moisture and wind speed contributions to the Vesta function (V). The wind speed term uses the near surface or 10 m wind (U_{10}, units $m\ s^{-1}$). The fuel moisture term is a function of relative humidity (RH, units %) and air temperature (T, units °C), which varies with time of day and time of year, expressed as three distinct periods (Eq. 7). Period 1 extends from midday to 5 PM from October to March. Period 2 is used otherwise for daylight hours, and Period 3 for night hours. Note, these periods are valid for southern hemisphere low- to mid-latitude regions. Application to the northern hemisphere, high latitudes requires additional consideration about when best to apply Period 1. (Experiments in the mid-summer Arctic, suggest Period 1 should apply continuously.)

For comparison with the better-known McArthur Forest Fire Danger Index (FFDI, McArthur 1967, Noble et al. 1980), $V = 15$ is roughly equivalent to an FFDI of 50, and $V = 30$ is similar to an FFDI of 100.

The PFT-flag is given by,

$$PFTflag = \frac{PFT}{V.U_{10}}. \quad 9.$$

To avoid divide by zero errors and to eliminate the PFT-flag triggering in light-wind conditions, or low fire danger conditions the PFT-flag is set to a very large number (to indicate pyroCb is impossible) whenever $V \leq 2.0$ or $U_{10} \leq 2.0$. The smaller the PFT-flag value, the more favourable the combined plume and fire conditions are for pyroCb formation. When calculating PFT-flag, PFT in units of GW is used in Eq. 9 to generate manageable PFT-flag units for plotting (e.g., Fig. 4).

Like the PFT, the PFT-flag is still in development and will undergo further tuning and editing in the future.

PFT-Flag results

A rigorous assessment of the PFT-flag is yet to be undertaken. At present a prediction of favourable pyroCb formation is based on a somewhat arbitrary choice of colour-scale in the PFT-flag plots. Both Sir Ivan and Licola yielded PFT-flag values between about 1 and 3 (Fig. 4), which led to the choice of a colour-scale between 0 and 5. Initial interpretation of these values is as follows: less than 1 is highly favourable for pyroCb formation; between 1 and 3 is favourable; between 3 and 5 is possible; and greater than 5 is unlikely. This is very preliminary and is likely to change in the future.

As mentioned above many cases have since been examined, with very promising results. A good example is the dual fires that produced pyroCb in view of the Mt. Hotham webcam on 4 March 2019: The Mayford-Tuckalong Track fire and the Mount Darling-Cynthia Range Track fire. Early in the day, while impressive pyroCu developed, there was no indication of pyroCb, and the PFT-flag indicated pyroCb was unlikely in the immediate vicinity of the fires (although favourable conditions were indicated nearby, Fig. 5). Throughout the afternoon, the PFT flag showed a steady southward progression of favourability, with the shading becoming increasingly darker (c.f., Figs 5 and 6). Both fires produced pyroCb, with the northern fire (Mayford-Tuckalong Track closest to the camera) triggering about an hour earlier than the southern fire.

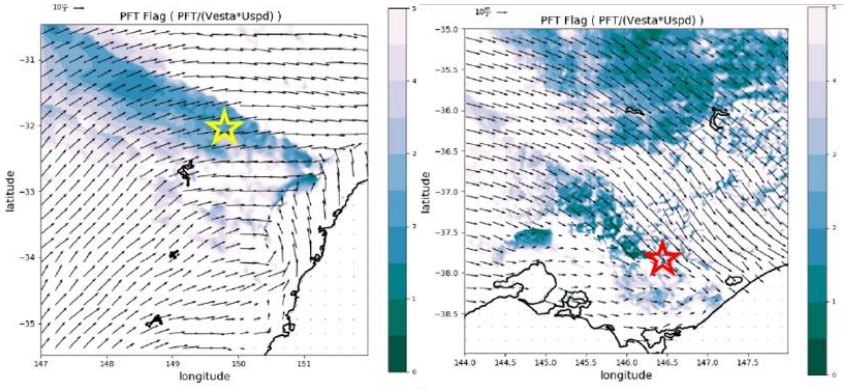

Figure 4: Same as Fig. 3 but PFT-flag forecasts. The stars indicate the fire locations.

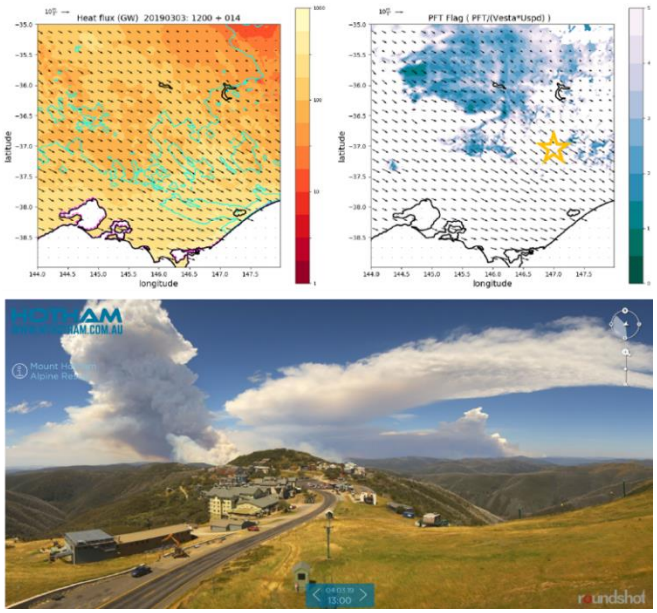

Figure 5: The PFT (top left), PFT-flag (top right) and below an image from the Mt. Hotham webcam of the Mayford-Tuckalong Track fire (left, mid-ground) and the Mount Darling-Cynthia Range Track fire (right, distant) at 1 PM, 4 March 2019. The star marks the location of the two fires.

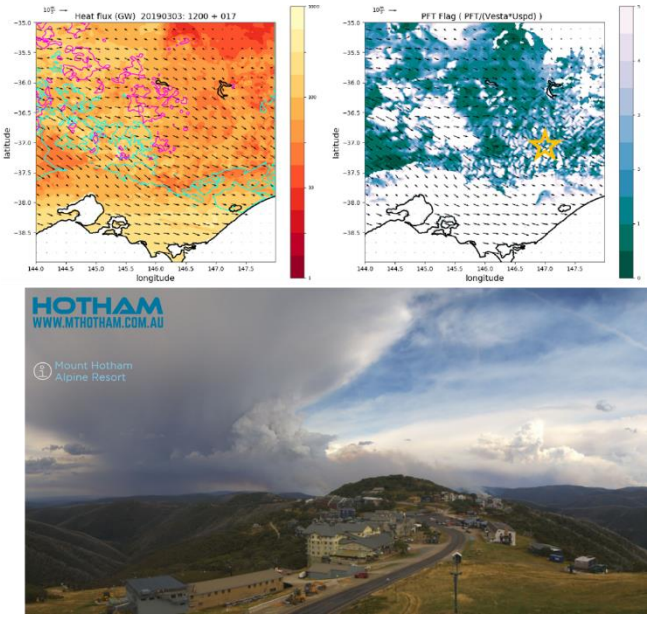

Figure 6: As in Fig. 5, but three hours later (4 PM).

The sequence of 10-minute images (not shown) showed the two plumes produced multiple bursts of deep convection throughout the afternoon, progressively becoming larger and more energetic, with clear evidence of rain falling from the nearby fire plume, and a mature anvil in the more remote fire plume. This behaviour was well-matched by the ever darkening and southward progression of the PFT-flag shading. As a forecast tool the PFT-flag would have provided excellent guidance for pyroCb prediction on these two fires.

Summary

A series of BNHCRC studies beginning with a little 'blue-sky' research into the thermodynamics of smoke plumes, led to the ability to identify potential condensation heights in plumes, and the minimum plume buoyancy required for plumes to freely convect to the electrification level. With this knowledge equations for a theoretical minimum firepower required for

pyroCb formation were derived using the Briggs plume model (PyroCb Firepower Threshold, PFT).

The work has culminated in the development of a diagnostic that seeks to determine when the atmosphere is conducive to both deep plume development and large, hot fires (PFT-flag). Originally designed as a flag to alert users when to examine the PFT, the PFT-flag may prove to be a more valuable prediction tool than the PFT itself. It was developed and tuned to identify the atmospheric conditions corresponding to two pyroCb events at opposite ends of the pyroCb spectrum. The first (Sir Ivan) occurred in catastrophic fire weather conditions, when pyroCb formation conditions were not especially favourable. The second (Licola) occurred in much milder fire weather conditions, when plume formation conditions were considerably more favourable. The PFT-flag has now been applied to more than 20 cases covering multiple days and time periods. While no rigorous performance assessment has yet been made the tool appears to be working surprisingly well. It not only identifies days of pyroCb occurrence, but also reproduces the diurnal variation in pyroCb threat, plus variations in threat associated with atmospheric features such as troughs, fronts and sea-breezes.

Both the PFT and PFT-flag are under continued development and will undergo real-time testing this coming southern Australian fire season.

Acknowledgements

Thanks to Mika Peace and Jeff Kepert for insightful comments and suggestions. Thanks also to Musa Kilinc for the webcam images.

References

Briggs, GA 1975, 'Plume rise predictions', Haugen, DA (eds), *Lectures on Air Pollution and Environmental Impact Analyses*, pp. 59—111, American Meteorology Society.

Briggs, GA 1984, 'Plume rise and buoyancy effects', Randerson, D (eds), *Atmospheric Science and Power Production*, US Dept of Energy DOE/TIC-27601, 327—366.

Cheney, NP, Gould, JS, McCaw, WL & Anderson, WR 2012, 'Predicting fire behaviour in dry eucalypt forest in southern Australia', *Forest Ecology and Management*, vol. 280, 120-131.

McArthur, A G, 1967, *Fire Behaviour in Eucalypt Forests,* Department of National Development Forestry and Timber Bureau, Canberra, Leaflet 107.

McRae, RHD & Sharples, JJ 2014, *Forecasting conditions conducive to blow-up fire events*, CAWCR Research Letters, Issue 11, 14--19. https://www.cawcr.gov.au/researchletters/CAWCR_Research_Letters_11.pdf

Noble, IR, Bary, GAV & Gill, AM 1980, 'McArthur's fire-danger meters expressed as equations', *Australian Journal of Ecology*, vol 5, 201-203pp.

Tory, KJ, Thurston, W & Kepert, JD 2018, 'Thermodynamics of pyrocumulus: A conceptual study', *American Meteorological Society*, vol 146, 2579--2598. DOI: 10.1175/MWR-D-17-0377.1

Tory, KJ & Kepert, JD 2018, 'Insights from the development of a pyrocumulonimbus prediction tool', *Proceedings from the Bushfire and Natural Hazards CRC Research Day*, AFAC conference, Perth, Australia, 2018, page 279. https://www.bnhcrc.com.au/sites/default/files/managed/downloads/annual_conference_proceedings_finalv3.pdf

Tory, KJ 2018, 'Models of buoyant plume rise', Bushfire and Natural Hazards CRC Report. https://www.bnhcrc.com.au/sites/default/files/managed/downloads/nb06-_1.1.1-modelsofbuoyantplumerisereviewbnhcrcstyle.pdf.